'89 KACC 1989. 10. 27~28

Robust Deterministic Control for Robotic Manipulators with Uncertainties

Chul Goo Kang, Roberto Horowitz and George Leitmann

Department of Mechanical Engineering
University of California at Berkeley
Berkeley, CA 94720, U.S.A.

A robust deterministic control for a class of singularly perturbed uncertain systems, where uncertainties are characterized deterministically rather than stochastically, is developed based mainly on information available on an uncertain reduced-order system. The deterministic control scheme is applied to the motion control of a n degree of freedom robotic manipulator. The parasitic actuator and sensor dynamics of the manipulator are explicitly considered in the stability analysis of the deterministic controller using a singular perturbation model. Simulation and experimental studies for a *two* degree of freedom, direct drive SCARA manipulator are conducted to evaluate the effectiveness of the derived control scheme.

1 Introduction

In recent years, considerable attention has been focused on the deterministic control of uncertain dynamical systems, where uncertainties are characterized deterministically rather than stochastically (see e.g. [1], [3], [4], [5], [7], [12], [13], [14], [15]). In [5], a class of singularly perturbed uncertain systems was considered, in which the system was decomposed into two coupled subsystems ("slow" and "fast" subsystems). The dynamics of the fast subsystem were characterized by means of a singular perturbation parameter μ. Smaller μ means faster response of the fast subsystem. A deterministic control was proposed based mainly on information available on the uncertain reduced-order system ($\mu = 0$). The deterministic control derived from this singular perturbation model is robust with respect to bounded uncertainties provided the "parasitic" dynamics are sufficiently small.

The application of robust deterministic control to robotic manipulators has been addressed by several authors (see e.g. [2], [4], [9], [16]). In [9], actual experimental results of a deterministic control applied to the positioning of a D.C. motor which has a time varying, uncertain inertia load, and Coriolis and friction disturbances, are presented. In all of the above mentioned implementation papers, the sensor and actuator "parasitic" dynamics are neglected in the controller design and in the stability analysis. However, some robotic systems, such as the one considered in this paper, have significant parasitic dynamics which may cause instability if their effect is neglected in the controller design.

The fact that the manipulator equations of motion are highly nonlinear, and that there may exist significant actuator and sensor parasitic dynamics, makes the control of these systems a challenging problem. In many applications, the exact inertial parameters of the manipulator may not be exactly known. Furthermore, exact decoupling control and cancellation of all dynamic disturbances in the equations of motion, such as Coriolis and gravitational disturbances, may not be computationally feasible. This is particularly true for systems in which the robot has six or more degrees of freedom. One way of solving these difficulties, as described in this paper, is to use a deterministic control law derived from a singular perturbation model, in which the actuator and sensor parasitic dynamics can be explicitly considered in the controller robustness analysis.

This paper is a revised version of [11] and includes experimental results. In this paper, the control scheme proposed in [5] is modified to make it more feasible to implement in robotic manipulator systems. Then the modified control scheme is applied to the tracking control of a robotic manipulator. The resulting continuous time controller is subsequently discretized and approximated using a zero-order hold. The performance of this deterministic control is evaluated by computer simulations and experiments for a two degree of freedom SCARA manipulator performing a typical pick-and-place task.

This paper is organized as follows. Section 2 presents the dynamic model of the manipulator used in this paper. In Section 3, the modified robust deterministic control scheme is briefly presented. In Section 4, an application method of the deterministic control to a n degree of freedom direct drive manipulator is shown. Section 5 presents the simulation and experimental results when the scheme in Section 4 is applied to a *two* degree of freedom direct drive SCARA manipulator. Conclusions are given in Section 6.

2 Dynamic model of a robotic manipulator

Consider the dynamics of n degree of freedom rigid link, direct drive manipulators with actuator and sensor parasitic dynamics. The input/output dynamics of these systems can be described in terms of the block diagram structure shown in Fig. 1. The manipulator dynamics are comprised of: Single Input Single Output (SISO) blocks which describe the actuator parasitic dynamics, SISO blocks which describe the velocity and position sensors parasitic dynamics, a Multi Input Multi Output (MIMO) block which describes the manipulator nonlinear rigid body dynamics, and pure integrator blocks which describe the input-output relations between joint velocities and positions.

The structure of the dynamic equations of motion for the manipulator nonlinear dynamics block is well known (cf. [8]). The equations of motion in the joint space can be expressed in the following form:

$$\mathbf{M}(\theta(t))\dot{\omega}(t) = \mathbf{q}(t) - \mathbf{v}(\theta(t), \omega(t)) - \mathbf{f}(\omega(t)) - \mathbf{g}(\theta(t)) \quad (2.1)$$

where $\theta(t)$ is the joint angular position vector, $\omega(t)$ is the joint angular velocity vector, $\mathbf{q}(t)$ is the torque vector supplied by the actuators, $\mathbf{M}(\theta(t))$ is the symmetric and positive definite generalized inertia matrix, $\mathbf{v}(\theta(t), \omega(t))$ is the vector due to Coriolis and centripetal accelerations, $\mathbf{f}(\omega(t))$ is the Coulomb friction torque vector and $\mathbf{g}(\theta(t))$ is the gravitational torque vector.

The robot considered in the simulation and experiment reported in this paper is a two degree of freedom direct drive SCARA manipulator. This arm was designed by the Department of Mechanical Engineering of the University of California at Berkeley and the Nippon Seiko K.K. (NSK) Corporation. This arm is generally referred to as the Berkeley/NSK manipulator. Fig. 2 shows the schematic diagram of the Berkeley/NSK manipulator. The manipulator consists of two NSK Megatorque motors, two NSK current amplifiers, two aluminium links, and two resolvers. The link dimensions and important model parameters of the Berkeley/NSK manipulator are given in Table 1. Note that gravitational torques are negligible in this manipulator.

To identify the sensor and actuator parasitic dynamics, the manipulator was disassembled into two motor/link subsystems with each motor attached to ground. Each motor/link subsystem was identified independently as a Single Input Single Output (SISO) linear system. For each axis, the overall open loop transfer function (from control input to sensor output) was identified from frequency response data using curve fitting of the magnitude and phase plots. Then the transfer function for each individual component was calculated based on the overall open loop transfer function and manufacturer's data. The identified transfer function for each actuator is first-order. The identified transfer functions for the velocity sensors of the base and second axes are seventh-order and tenth-order, respectively. The identified transfer functions for the position sensors for both axes are third-order. For more details regarding the modelling and identification of the dynamics, and for the specific transfer function of each component, refer to [10].

Additional nonlinear effects such as Coulomb friction, actuator saturation, sensor noise, and quantization effects are also considered in the model. Complete modelling details are found in [10].

3 A robust deterministic control

When the deterministic control scheme proposed in [5] is applied to a robotic manipulator, and the structure described in the previous section is used to model the system, the control law becomes linear and the imposed conditions are unduly conservative. In this section we will present a modified control scheme which allows both linear and nonlinear control action and which relaxes some of the conditions of the control scheme proposed in [5]. The modified control scheme proposed is a deterministic output feedback control based on a singular perturbation model and knowledge of the bounds of the system uncertainties. The full development of this control law and a complete stability analysis will be given in a forthcoming paper.

The class of *full-order* systems to be considered is represented by the following singular perturbation model:

$$\begin{aligned}\dot{\mathbf{x}}(t) &= \mathbf{A}_{11}\mathbf{x}(t) + \mathbf{A}_{12}\mathbf{y}(t) + \mathbf{B}_1\mathbf{u}(t) \\ &\quad + \mathbf{g}_1(t, \mathbf{x}(t), \mathbf{y}(t), \mathbf{u}(t)) \qquad (3.2)\end{aligned}$$

$$\mathbf{x}(t) \in \mathbf{R}^n, \mathbf{u}(t) \in \mathbf{R}^m$$

$$\begin{aligned}\mu\dot{\mathbf{y}}(t) &= \mathbf{F}[\mathbf{A}_{21}\mathbf{x}(t) + \mathbf{y}(t) + \mathbf{B}_2\mathbf{u}(t)] \\ &\quad + \mathbf{g}_2(t, \mathbf{x}(t), \mathbf{y}(t), \mathbf{u}(t), \mu) \qquad (3.3) \\ \mathbf{y}(t) &\in \mathbf{R}^p, \mu \in (0, \infty)\end{aligned}$$

with output

$$\mathbf{z}(t) = \mathbf{S}\mathbf{x}(t) + \mathbf{C}\mathbf{y}(t), \ \mathbf{z}(t) \in \mathbf{R}^n, \qquad (3.4)$$

where $\mathbf{A}_{ij}, \mathbf{B}_i, \mathbf{F}$, $\mathbf{S}$ and $\mathbf{C}$ are known constant real matrices, and $\mathbf{g}_1$ and $\mathbf{g}_2$ are uncertain Carathéodory functions.[1] The subsystem described by Eq. (3.2) is referred to as the *slow* subsystem, while the subsystem described by Eq. (3.3) is referred to as the *fast* subsystem. Notice that the singular perturbation parameter μ in Eq. (3.3) is used as a measure of the speed of the response of the fast subsystem. Smaller μ means faster response.

The following set of assumptions concerning the fast subsystem are required in our control formulation:

Assumption 1 :

(i) $\mathbf{F}$ is a stable matrix, i.e., all eigenvalues $\lambda(\mathbf{F}) \subset \mathbf{C}^-$ (the open left half complex plane) .

(ii) $\mathbf{g}_2(t, \mathbf{x}, \mathbf{y}, \mathbf{u}, 0) = \mathbf{0} \ \forall (t, \mathbf{x}, \mathbf{y}, \mathbf{u}) \in \mathbf{R} \times \mathbf{R}^n \times \mathbf{R}^p \times \mathbf{R}^m$.

We now define the *reduced-order* system which is derived from the full-order system by letting the perturbation parameter $\mu = 0$. When $\mu = 0$, the fast subsystem Eq. (3.3) reduces to the algebraic equation

$$\mathbf{y}(t) = -\mathbf{A}_{21}\mathbf{x}(t) - \mathbf{B}_2\mathbf{u}(t) \triangleq \mathbf{H}(\mathbf{x}(t), \mathbf{u}(t)),$$

and the following reduced-order system is obtained:

$$\dot{\mathbf{x}}(t) = \bar{\mathbf{A}}\mathbf{x}(t) + \bar{\mathbf{B}}\mathbf{u}(t) + \bar{\mathbf{g}}(t, \mathbf{x}(t), \mathbf{u}(t)), \qquad (3.5)$$

where $\bar{\mathbf{A}} \triangleq \mathbf{A}_{11} - \mathbf{A}_{12}\mathbf{A}_{21}$, $\bar{\mathbf{B}} \triangleq \mathbf{B}_1 - \mathbf{A}_{12}\mathbf{B}_2$, $\bar{\mathbf{g}}(t, \mathbf{x}, \mathbf{u}) \triangleq \mathbf{g}_1(t, \mathbf{x}, \mathbf{H}(\mathbf{x}, \mathbf{u}))$.

The following set of assumptions concerning the reduced-order system are required in our control formulation:

Assumption 2 :

(i) The pair $(\bar{\mathbf{A}}, \bar{\mathbf{B}})$ is stabilizable.

(ii) $\mathbf{S} - \mathbf{C}\mathbf{A}_{21} = \mathbf{I}$.

(iii) $\mathbf{C}\mathbf{B}_2 = \mathbf{0}$.

From (ii) and (iii) in Assumption 2, the output equation (3.4) for the reduced-order system reduces to

$$\mathbf{z}(t) = \mathbf{x}(t). \qquad (3.6)$$

We now define a set of design parameters $(\mathbf{Q}, \gamma_0) \in \mathbf{R}^{n \times n} \times \mathbf{R}^+$ ($\mathbf{R}^+ \triangleq [0, \infty)$) which have the following properties:

(i) $\mathbf{Q}$ is symmetric and positive definite.

(ii) $\gamma_0 > 0$ if $\lambda(\bar{\mathbf{A}}) \not\subset \mathbf{C}^-$.

Let $\mathbf{K} \in \mathbf{R}^{n \times n}$ be the unique positive definite and symmetric solution of the following Riccatti equation:

$$\mathbf{K}\bar{\mathbf{A}} + \bar{\mathbf{A}}^T\mathbf{K} + \mathbf{Q} - 2\gamma_0\mathbf{K}\bar{\mathbf{B}}\bar{\mathbf{B}}^T\mathbf{K} = \mathbf{0} \qquad (3.7)$$

[1] The definition of Carathéodory function is given in reference [7]; note that a continuous function is Carathéodory.

Assumption 3 :

There exist known non-negative real numbers $\alpha_1, \alpha_2, \alpha_3$, α_4 and β, with $\beta < 1$, and unknown Carathéodory functions $\mathbf{d}, \mathbf{e} : \mathbf{R} \times \mathbf{R}^n \times \mathbf{R}^m \to \mathbf{R}^n$, such that

(i) $\bar{\mathbf{g}}(t, \mathbf{x}, \mathbf{u}) = \bar{\mathbf{B}}\mathbf{e}(t, \mathbf{x}, \mathbf{u}) + \mathbf{d}(t, \mathbf{x}, \mathbf{u})$

(ii) $\|\mathbf{d}(t, \mathbf{x}, \mathbf{u})\| \leq \alpha_1 \|\mathbf{x}\| + \alpha_2$

(iii) $\|\mathbf{e}(t, \mathbf{x}, \mathbf{u})\| \leq \alpha_3 \|\mathbf{x}\| + \alpha_4 + \beta \|\mathbf{u}\|$

(iv) $\alpha_1 + \alpha_3 \|\bar{\mathbf{B}}\| < \frac{\lambda_{min}(\mathbf{Q}\mathbf{K}^{-1})}{2\, \|\mathbf{K}\|^{1/2} \|\mathbf{K}^{-1}\|^{1/2}}$.

Define two sets, Γ_1, $\Gamma_2 \in \mathbf{R}$ as

$$\Gamma_1 \triangleq (\underline{\gamma}, \infty), \quad \underline{\gamma} \triangleq (1 - \beta)^{-1} \gamma_0,$$

$$\Gamma_2 \triangleq \{\gamma \in [0, \infty) : \tilde{\mathbf{F}}(\gamma) \text{ is stable}\}$$

where $\tilde{\mathbf{F}}(\gamma) \triangleq \mathbf{F}[\mathbf{I} - \gamma \mathbf{B}_2 \bar{\mathbf{B}}^T \mathbf{K} \mathbf{C}]$.

Assumption 4 :

$$\Gamma^* \triangleq \Gamma_1 \cap \Gamma_2 \neq \emptyset$$

Feedback control law

Choose $\epsilon > 0$ as another design parameter. Now the following nonlinear output feedback control law is proposed:

$$\mathbf{u}(t) = \mathbf{p}(\mathbf{z}(t)) \tag{3.8}$$

$$\mathbf{p}(\mathbf{z}(t)) = \mathbf{p}_l(\mathbf{z}(t)) + \mathbf{p}_n(\mathbf{z}(t)). \tag{3.9}$$

The linear component $\mathbf{p}_l(\mathbf{z}(t))$ is defined by

$$\mathbf{p}_l(\mathbf{z}(t)) \triangleq -\gamma_1 \bar{\mathbf{B}}^T \mathbf{K} \mathbf{z}(t), \ \gamma_1 \in \Gamma^*. \tag{3.10}$$

The nonlinear component $\mathbf{p}_n(\mathbf{z}(t))$ is defined by

$$\mathbf{p}_n(\mathbf{z}(t)) \triangleq -\frac{\bar{\mathbf{B}}^T \mathbf{K} \mathbf{z}(t)}{\|\bar{\mathbf{B}}^T \mathbf{K} \mathbf{z}(t)\| + \epsilon} \rho, \tag{3.11}$$

where ρ is yet another design parameter satisfying

$$0 \leq \rho < \frac{\epsilon}{2\, \|\mathbf{P}\mathbf{F}\mathbf{B}_2 \bar{\mathbf{B}}^T \mathbf{K}\|\, \|\mathbf{C}\|}, \tag{3.12}$$

and $\mathbf{P} \in \mathbf{R}^{p \times p}$ is the positive definite, symmetric solution of

$$\mathbf{P}\tilde{\mathbf{F}}(\gamma_1) + \tilde{\mathbf{F}}(\gamma_1)^T \mathbf{P} = -\mathbf{I}.$$

Notice that the control law presented above is formulated mainly on information available from the reduced-order system in Eq. (3.5) and on knowledge of the bound on the norm of the uncertainty $\bar{\mathbf{g}}(t, \mathbf{x}, \mathbf{u})$.

With this output feedback control, the reduced-order system (3.5) is *globally uniformly attractive*.[2] The derivation of this result will be presented in a forthcoming paper. Defining

$$\mathbf{h}(\mathbf{x}) \triangleq \mathbf{H}(\mathbf{x}, \mathbf{p}(\mathbf{x})) = -\mathbf{A}_{21}\mathbf{x} - \mathbf{B}_2 \mathbf{p}(\mathbf{x}),$$

a final assumption concerning the robustness of the control with the full-order system is made:

Assumption 5 :

(i) For all $(t, \mathbf{x}) \in \mathbf{R} \times \mathbf{R}^n$,

$$\|\mathbf{g}_1(t, \mathbf{x}, \mathbf{y}_1, \mathbf{p}(\mathbf{S}\mathbf{x} + \mathbf{C}\mathbf{y}_1)) - \mathbf{g}_1(t, \mathbf{x}, \mathbf{y}_2, \mathbf{p}(\mathbf{S}\mathbf{x} + \mathbf{C}\mathbf{y}_2))\| \leq \lambda(\mathbf{y}_1 - \mathbf{y}_2), \ \forall\, \mathbf{y}_1, \mathbf{y}_2 \in \mathbf{R}^p$$

where $\lambda \geq 0$ is a known constant.

(ii) For all $(t, \mathbf{x}, \mathbf{y}) \in \mathbf{R} \times \mathbf{R}^n \times \mathbf{R}^p$ and $\mu \geq 0$,

$$\|\mathbf{g}_2(t, \mathbf{x}, \mathbf{y}, \mathbf{p}(\mathbf{S}\mathbf{x} + \mathbf{C}\mathbf{y}), \mu)\| \leq \mu\, [\kappa_1 \|\mathbf{y} - \mathbf{h}(\mathbf{x})\| + \kappa_2 \|\mathbf{x}\| + \kappa_3],$$

where $\kappa_1, \kappa_2, \kappa_3 \geq 0$ are known constants.

With the addition of Assumption 5, it is assured that there exists a calculable $\mu^* > 0$ such that, for $\mu \in (0, \mu^*)$, the full-order system subject to the controller (3.8) is *globally uniformly attractive*. The derivation of this result will be presented in a forthcoming paper.

4 Application of the control to a robotic manipulator

This section presents an application method of the deterministic control scheme proposed in Section 3 to the tracking control of an n degree of freedom robotic manipulator. The control objective is to follow a desired trajectory which is defined in terms of desired joint position and velocity vectors, denoted respectively by $\theta_d(t)$ and $\omega_d(t)$. Since the control scheme in Section 3 is the one for regulation, it must be slightly modified to be applied to the tracking control of the robotic manipulator. The block diagram of the control scheme, as an application method, is shown in Fig. 3.

In the remainder of this section, we will show how the control system in Fig. 3 can be formulated in terms of the singular perturbation full-order model described in Section 3. We begin by defining the state vector $\mathbf{x}(t)$ of the slow subsystem in Eq. (3.2) and the output vector $\mathbf{z}(t)$ of the system in Eq. (3.4) as follows:

$$\mathbf{x}(t) \triangleq \begin{bmatrix} \theta_d(t) - \theta(t) \\ \omega_d(t) - \omega(t) \end{bmatrix} \triangleq \begin{bmatrix} \mathbf{x}_\theta(t) \\ \mathbf{x}_\omega(t) \end{bmatrix} \tag{4.13}$$

$$\mathbf{z}(t) \triangleq \begin{bmatrix} \hat{\theta}_d(t) - \hat{\theta}(t) \\ \hat{\omega}_d(t) - \hat{\omega}(t) \end{bmatrix} \triangleq \begin{bmatrix} \mathbf{z}_\theta(t) \\ \mathbf{z}_\omega(t) \end{bmatrix}, \tag{4.14}$$

$\theta_d(t)$ is the desired joint position vector, and $\omega_d(t)$ is the desired joint velocity vector. $\theta(t)$ is the joint position vector and $\omega(t)$ is the joint velocity vector. $\hat{\theta}(t)$ is the measured joint position vector, i.e., the outputs of position sensors, $\hat{\omega}(t)$ is the measured joint velocity vector, i.e., the outputs of velocity sensors. $\hat{\theta}_d(t)$ is the filtered desired position vector, i.e., the prefilter output of $\theta_d(t)$, and $\hat{\omega}_d(t)$ is the filtered desired velocity vector, i.e., the prefilter output of $\omega_d(t)$. For convenience, $\mathbf{x}(t)$ is divided into the two sub-vectors $\mathbf{x}_\theta(t)$ and $\mathbf{x}_\omega(t)$, and $\mathbf{z}(t)$ into the two sub-vectors $\mathbf{z}_\theta(t)$ and $\mathbf{z}_\omega(t)$.

Let the transfer function matrices of the position and velocity sensors be denoted by $G_\theta(s)$ and $G_\omega(s)$, respectively. The measured position and velocity vectors can be expressed by

$$\hat{\theta}(s) = G_\theta(s)\theta(s)$$
$$\hat{\omega}(s) = G_\omega(s)\omega(s).$$

Define the filters of the desired positions and velocities, denoted by $G_{\theta_d}(s)$ and $G_{\omega_d}(s)$, as some convenient factor of $G_\theta(s)$ and $G_\omega(s)$, respectively. The filtered desired position and velocity vectors can be expressed by

$$\hat{\theta}_d(s) = G_{\theta_d}(s)\theta_d(s)$$
$$\hat{\omega}_d(s) = G_{\omega_d}(s)\omega_d(s).$$

In the Laplace transform domain, the two output sub-

[2] The definition of a global uniform attractor is given in reference [5].

vectors $\mathbf{z}_\theta(t)$ and $\mathbf{z}_\omega(t)$ can be written as follows:

$$\begin{aligned}\mathbf{z}_\theta(s) &= G_\theta(s)[\theta_d(s)-\theta(s)] + [G_{\theta_d}(s)-G_\theta(s)]\theta_d(s)\\ &= \mathbf{z}_1(s)+\mathbf{z}_2(s)\end{aligned}$$

where

$$\mathbf{z}_1(s) \triangleq G_\theta(s)[\theta_d(s)-\theta(s)] \tag{4.15}$$

$$\mathbf{z}_2(s) \triangleq [G_{\theta_d}(s)-G_\theta(s)]\theta_d(s) \triangleq \Delta G_\theta(s)\theta_d(s), \tag{4.16}$$

and

$$\begin{aligned}\mathbf{z}_\omega(s) &= G_\omega(s)[\omega_d(s)-\omega(s)] + [G_{\omega_d}(s)-G_\omega(s)]\omega_d(s)\\ &= \mathbf{z}_3(s)+\mathbf{z}_4(s)\end{aligned}$$

where

$$\mathbf{z}_3(s) \triangleq G_\omega(s)[\omega_d(s)-\omega(s)] \tag{4.17}$$

$$\mathbf{z}_4(s) \triangleq [G_{\omega_d}(s)-G_\omega(s)]\omega_d(s) \triangleq \Delta G_\omega(s)\omega_d(s). \tag{4.18}$$

The following state space realizations can be defined for the transfer function matrices in equations (4.15) and (4.17):

$$\begin{aligned}\mathbf{z}_1(t) &= \mathbf{C}_\theta \mathbf{y}_\theta(t)\\ \dot{\mathbf{y}}_\theta(t) &= \mathbf{F}_\theta \mathbf{y}_\theta(t) + \mathbf{B}_\theta \mathbf{x}_\theta(t),\end{aligned} \tag{4.19}$$

$$\begin{aligned}\mathbf{z}_3(t) &= \mathbf{C}_\omega \mathbf{y}_\omega(t)\\ \dot{\mathbf{y}}_\omega(t) &= \mathbf{F}_\omega \mathbf{y}_\omega(t) + \mathbf{B}_\omega \mathbf{x}_\omega(t),\end{aligned} \tag{4.20}$$

where $\mathbf{F}_\theta$ and $\mathbf{F}_\omega$ are chosen to be block-diagonal matrices.

Similar to the sensor parasitic dynamics, the input-output relations for the actuator parasitic dynamics can be expressed by

$$\mathbf{q}(s) = G_a(s)\mathbf{u}(s),$$

with the following state space realization:

$$\dot{\mathbf{q}}(t) = \mathbf{F}_a \mathbf{q}(t) + \mathbf{B}_a \mathbf{u}(t), \tag{4.21}$$

where $\mathbf{F}_a$ is chosen as a block-diagonal matrix.

Define the singular perturbation parameter μ as the inverse of the smallest absolute value of the real part among the eigenvalues of $\mathbf{F}_\theta, \mathbf{F}_\omega$ and $\mathbf{F}_a$ in Eqs. (4.19), (4.20) and (4.21).

Equation (4.16) can be written as

$$\mathbf{z}_2(s) = \Delta G_\theta(s)\theta_d(s) \triangleq \Delta G_{1\theta}(s)\Delta G_{2\theta}(s,\mu)\theta_d(s), \tag{4.22}$$

where $\Delta G_{2\theta}(s,0) = 0$. This condition may be satisfied by selecting $\Delta G_{1\theta}(s) = G_{\theta_d}(s)$ and, as previously mentioned, selecting $G_{\theta_d}(s)$ as a factor of $G_\theta(s)$. A state space realization for Eq. (4.22) can be defined by

$$\begin{aligned}\mathbf{z}_2(t) &= \mathbf{C}_{\tilde{\theta}} \mathbf{y}_{\tilde{\theta}}(t)\\ \dot{\mathbf{y}}_{\tilde{\theta}} &= \mathbf{F}_{\tilde{\theta}} \mathbf{y}_{\tilde{\theta}}(t) + \mathbf{B}_{\tilde{\theta}} \mathbf{g}_{21}(t,\mu)\end{aligned} \tag{4.23}$$

where $\mathbf{g}_{21}(t,\mu) = \mathcal{L}^{-1}\{\Delta G_{2\theta}(s,\mu)\theta_d(s)\}$ and $\mathcal{L}^{-1}$ denotes the inverse Laplace transform operator. As in previous cases, $\mathbf{F}_{\tilde{\theta}}$ is selected to be a block-diagonal matrix.

Similarly, Eq. (4.18) can be expressed as

$$\mathbf{z}_4(s) = \Delta G_\omega(s)\omega_d(s) \triangleq \Delta G_{1\omega}(s)\Delta G_{2\omega}(s,\mu)\omega_d(s),$$

where $\Delta G_{2\omega}(s,0) = 0$, and realized in the state space as

$$\begin{aligned}\mathbf{z}_4(t) &= \mathbf{C}_{\tilde{\omega}} \mathbf{y}_{\tilde{\omega}}(t)\\ \dot{\mathbf{y}}_{\tilde{\omega}}(t) &= \mathbf{F}_{\tilde{\omega}} \mathbf{y}_{\tilde{\omega}}(t) + \mathbf{B}_{\tilde{\omega}} \mathbf{g}_{22}(t,\mu),\end{aligned} \tag{4.24}$$

where $\mathbf{g}_{22}(t,\mu) = \mathcal{L}^{-1}\{\Delta G_{2\omega}(s,\mu)\omega_d(s)\}$. Note that $\mathbf{g}_{2i}(t,0) = 0$, $i = 1,2$. For given $\mu \in (0,\infty)$, $\mathbf{g}_{2i}(t,\mu)$ is bounded, since $\Delta G_{2\theta}(s,\mu)$ and $\Delta G_{2\omega}(s,\mu)$ are stable transfer functions, and $\theta_d(t)$ and $\omega_d(t)$ are assumed to be bounded.

Defining the state vector of the fast subsystem, $\mathbf{y}(t)$, by

$$\mathbf{y}^T(t) \triangleq [\mathbf{y}_\theta^T(t), \mathbf{y}_{\tilde{\theta}}^T(t), \mathbf{y}_\omega^T(t), \mathbf{y}_{\tilde{\omega}}^T(t), \mathbf{q}^T(t)], \tag{4.25}$$

and using the definitions for the state vector of the slow subsystem, $\mathbf{x}(t)$, and output vector $\mathbf{z}(t)$ in Eqs. (4.13) and (4.14), respectively, equations (4.19), (4.20), (4.21), (4.23) and (4.24) can be collected into the following single state space formulation:

$$\begin{aligned}\mu\dot{\mathbf{y}}(t) &= \mathbf{F}[\mathbf{A}_{21}\mathbf{x}(t) + \mathbf{y}(t) + \mathbf{B}_2\mathbf{u}(t)]\\ &\quad + \mathbf{g}_2(t,\mathbf{x}(t),\mathbf{y}(t),\mu)\\ \mathbf{z}(t) &= \mathbf{C}\mathbf{y}(t)\end{aligned} \tag{4.26}$$

where $\mathbf{F}, \mathbf{A}_{21}, \mathbf{B}_2$ and $\mathbf{C}$ are real matrices of appropriate dimensions.

We will now derive the corresponding state equation for the slow subsystem, Eq. (3.2), using the nonlinear manipulator equations of motion, Eq. (2.1). Eq. (2.1) can be written as

$$\dot{\omega}(t) = \mathbf{B}(\theta(t))[\mathbf{q}(t) - \mathbf{v}(\theta(t),\omega(t)) - \mathbf{f}(\omega(t))]. \tag{4.27}$$

where $\mathbf{B}(\theta) \triangleq \mathbf{M}^{-1}(\theta) \triangleq \mathbf{B}_o[\mathbf{I} + \mathbf{E}(\theta)]$ with

$$\mathbf{B}_o \triangleq \frac{\max_\theta\{\lambda_{max}(\mathbf{B}(\theta))\} + \min_\theta\{\lambda_{min}(\mathbf{B}(\theta))\}}{2}, \tag{4.28}$$

and $\lambda_{max}(\mathbf{B}(\theta))$ and $\lambda_{min}(\mathbf{B}(\theta))$ are the maximum and minimum eigenvalues of $\mathbf{B}(\theta)$. Note that definition (4.28) guarantees that $\beta = max\|\mathbf{E}(\theta)\| < 1$, which is the required for the satisfaction of Assumption 3 (iv) in Section 3.

Equation (4.27) can be rewritten as

$$\dot{\omega}(t) = \mathbf{B}_o\mathbf{q}(t) + \mathbf{B}_o\mathbf{E}(\theta)\mathbf{q}(t) - \mathbf{B}(\theta)[\mathbf{v}(\theta,\omega) + \mathbf{f}(\omega)]. \tag{4.29}$$

Using the definitions of $\mathbf{x}(t)$ given in Eq. (4.13) and of $\mathbf{y}(t)$ given in Eq. (4.25), the following state equation is derived from Eq. (4.29):

$$\dot{\mathbf{x}}(t) = \mathbf{A}_{11}\mathbf{x}(t) + \mathbf{A}_{12}\mathbf{y}(t) + \mathbf{g}_1(t,\mathbf{x}(t),\mathbf{y}(t)) \tag{4.30}$$

where

$$\mathbf{g}_1(t,\mathbf{x},\mathbf{y}) = \begin{bmatrix} 0 \\ \dot{\omega}_d(t) - \mathbf{B}_o\mathbf{E}(\theta)\mathbf{q}(t) + \mathbf{B}(\theta)[\mathbf{v}(\theta,\omega) + \mathbf{f}(\omega)] \end{bmatrix}. \tag{4.31}$$

$\mathbf{A}_{11}$ and $\mathbf{A}_{12}$ are real matrices of appropriate dimensions.

The system described by equations (4.26) and (4.30) is included in the class of systems considered in Section 3. Furthermore, it can be shown that every assumption in Section 3 is satisfied except that α_4 in Assumption 3 (iii) depends on $\mathbf{x}(t)$ and t. This is due to the fact that the Coriolis term $\mathbf{v}(\theta,\omega)$ in Eq. (4.31) is a quadratic function of the manipulator's joint velocity vector ω. Let us assume that $\mathbf{v}(\theta,\omega)$ can be approximated by $\mathbf{v}(\theta_d,\omega_d)$; then, α_4 can be considered constant since θ_d is bounded. With this assumption, the manipulator system described by Eqs. (4.26) and (4.30) satisfies all of the assumptions in Section 3, and the deterministic control law (3.8) can be applied to this system.

5 Simulation and experimental results

The formulation in Section 4 was applied to a *two* degree of

freedom direct drive SCARA manipulator (Berkeley/NSK manipulator), and computer simulation and experimental studies were conducted to test and evaluate the proposed deterministic control scheme. Details on the computer simulation model and the real system used can be found in reference [10].

The desired trajectory for both axes is given by a seventh order polynomial, simulating a pick-and-place operation. Fig. 4 shows the desired trajectory and the payload changes.

The existence of μ^*, which is the upper limit of the singular perturbation parameter μ that assures a stable control system, was shown in successive numerical simulations. Since the theory in Section 3 is conservative, the μ^* calculated from it is too small; thus, to obtain a less conservative value of μ^*, we used simulation tests. Simulation tests were performed by artificially increasing the values of μ until the feedback system became unstable. These results are shown in Fig. 5 in which the system is stable for $\mu = 2 \times 7.55 \times 10^{-4}$, but the system becomes unstable for $\mu = 4 \times 7.55 \times 10^{-4}$. Thus, μ^* lies between $2 \times 7.55 \times 10^{-4}$ and $4 \times 7.55 \times 10^{-4}$. The actual fast subsystem of the Berkeley/NSK manipulator has a value of $\mu = 7.55 \times 10^{-4}$; thus, $\mu < \mu^*$. The design parameters in Fig. 5 were $\mathbf{Q} = diag(180, 5, 135, 0.1)$, $\gamma_0 = 0.013$, $\gamma_1 = 1$, $\epsilon = 80$, $\rho = 100$.

To investigate the possibility of implementing the control law with a digital computer, the continuous time control was discretized and approximated by a zero-order hold. The design parameters used in the simulations and the experiments of the discretized control were $\mathbf{Q} = diag(16000, 5, 170, 0.1)$, $\gamma_0 = 0.13$, $\gamma_1 = 5.8$, $\epsilon = 40$, $\rho = 50$. The set Γ^* defined in Assumption 4 in Section 3 is the interval $(5.2, \infty)$ in these design parameters; however, the upper limit of Γ^* is bounded by the condition that $\mu^* > \mu$. Fig. 6, Fig. 7 and Fig. 8 show the simulation results for the position trackings, position tracking errors and the control inputs of both axes when the discrete control is used with sampling time = 8 ms, payload = 0 and computational delay = 3.8 ms. The 3.8 ms is the actual time required to execute all the calculations of the control algorithm with an IBM-AT (80286-10 MHz, 80287-5 MHz). The tracking errors and control inputs in Fig. 7 and Fig. 8 are close to the ones when the continuous time control is used. Nonlinearities such as torque saturations of the actuators, voltage saturations of the D/A converters, quantization effects, as well as the nonlinear manipulator dynamics, were considered in the simulation,

Fig. 9 shows the position tracking errors for the experiment which uses exactly the same design parameters used in the simulation (See Fig. 7). Fig. 7 and Fig. 9 show the tracking error trends are consistent in the simulation and the experiment.

When the task is executed with picking up the 6.8 Kg payload, the tracking errors become bigger. The results of this simulation are shown in Fig. 10 and Fig. 11. Notice that, when the payload is between zero and 6.8 Kg, the control system is always stable. In other words, the proposed control scheme is robust with respect to payload variations.

If the tracking errors are too big, they can be made smaller by reducing ϵ in Eq. (3.11) and adjusting other design parameters, provided that chattering of input signals can be endured. The control can be made linear by setting $\rho = 0$ in Eq. (3.11). However, the combination of linear and nonlinear control provides the control engineer with more flexibility in tuning the controller for better performance.

When the computational delay is included in this deterministic control scheme, the control system generally chatters. This is one motivation for deriving a digital version of this control scheme such as the one presented in [6].

6 Conclusions

This paper presents the application of a deterministic control to a robotic manipulator. The robustness of the control system to neglected actuator and sensor parasitic dynamics, as well as variations in the manipulator payload, and other parametric uncertainties, is explicitly considered in the stability analysis. The control law is a modification of the deterministic control for singularly perturbed uncertain systems, originally introduced in [5]. The modifications introduced in this paper relax some of the conditions required in [5], simplify the controller design, and make the overall control scheme more practical when applied to robotic manipulators.

Simulation and experimental studies were conducted to evaluate the performance of the proposed deterministic control scheme for the two degree of freedom, direct drive SCARA manipulator (Berkeley/NSK manipulator) in [10]. The simulation and experimental results show that: (i) the deterministic control scheme proposed in this paper is effective for the tracking control of a robotic manipulator, (ii) the controller is robust with respect to payload variations and varying inertia, and (iii) the experimental result is consistent with the simulation result.

The application of the control scheme presented in this paper is specific to the control of a n degree of freedom direct drive robotic manipulator. However, it can be used to control any general n degree of freedom robotic manipulators or other mechanical systems where parasitic dynamics are present and the measurement or calculation of the varying system parameters is not practical. The development of the digital version of the deterministic control scheme is another topic for more study.

Acknowledgements

This work was supported by the National Science Foundation under grant MSM-8657520 and grant ECS-8602524.

References

[1] G. Ambrosino, G. Celentano, and F. Garofalo. Robust model tracking control for a class of nonlinear plants. *IEEE Trans. Automat. Contr.*, AC-30:275–279, 1985.

[2] Y. H. Chen. Robust control of mechanical manipulators. *ASME J. Dynam. Syst. Meas. Contr.*, submitted.

[3] M. Corless and G. Leitmann. Continuous state feedback guaranteeing uniform ultimate boundedness for uncertain dynamic systems. *IEEE Trans. Automat. Contr.*, 26:1139–1144, 1981.

[4] M. Corless and G. Leitmann. Deterministic control of uncertain systems. *Proc. American Control Conf.*, :2019–2025, June, 1988. Atlanta, Georgia.

[5] M. Corless, G. Leitmann, and E. P. Ryan. Control of uncertain systems with neglected dynamics. *Deterministic Nonlinear Control of Uncertain Systems: Variable Structure and Lyapunov Control, ed., A. Zinober*, to appear. IEE Publ., London.

[6] M. Corless and J. Manela. Control of uncertain discrete-time systems. *Proc. American Control Conf.*, 1986. Seattle, Washington.

[7] M. Corless and E. P. Ryan. Robust feedback control of a class of singularly perturbed uncertain dynamical systems. *Proc. IEEE Conf. Decision Control*, :1684–1686, 1988. Austin, Texas.

[8] John J. Craig. *Introduction to Robotics: Mechanics and Control.* Addison-Wesley Publ. Co., 1986.

[9] R. Horowitz, H. Stephens, and G. Leitmann. Experimental verification of a deterministic controller for a d.c. motor with uncertain dynamics. *Proc. American Control Conf.*, June, 1987. Minneapolis, MN.

[10] C. G. Kang, W. W. Kao, M. Boals, and R. Horowitz. Modeling, identification and simulation of a two link Scara manipulator. *Proc. Winter Annual Meeting of ASME: Symposium on Robotics*, :393-407, Nov., 1988. Chicago, IL.

[11] C. G. Kang, G. Leitmann, and R. Horowitz. Robust deterministic controller design of a two degree of freedom SCARA manipulator. *Proc. American Control Conf.*, :1457–1462, 1989. Pittsburgh, PA.

[12] G. Leitmann. Deterministic control of uncertain systems. *Astronautica Acta*, 7:1457–1461, 1980.

[13] G. Leitmann. On the efficacy of nonlinear control in uncertain linear systems. *ASME J. Dynam. Syst. Meas. Contr.*, 103:95–102, 1981.

[14] G. Leitmann and E. P. Ryan. Output feedback control of a class of singularly perturbed uncertain dynamical systems. *Proc. American Control Conf.*, :1590–1594, June, 1987. Minneapolis, MN.

[15] G. Leitmann, E. P. Ryan, and A. Steinberg. Feedback control of uncertain systems: robustness with respect to neglected actuator and sensor dynamics. *Int. J. Control*, 43:1243–1256, 1986.

[16] R. Shoureshi, M. Corless, and M. D. Roesler. Control of industrial manipulator with bounded uncertainties. *ASME J. Dynam. Syst. Meas. Contr.*, 109:53–59, 1987.

Table 1 The dimensions and the parameters of the Berkeley/NSK manipulator

rotor inertia of base motor	0.2675 Kg·m
base link inertia about center of gravity(c.g.)	0.360 Kg·m
rotor inertia of second motor	0.0077 Kg·m
stator inertia of second motor	0.040 Kg·m
second link inertia about c.g.	0.051 Kg·m
payload inertia about c.g.	0.046 Kg·m
base motor mass	73.0 Kg
base link mass	10.6 Kg
second motor mass	12.0 Kg
second link mass	4.85 Kg
payload mass	6.81 Kg
base link length	0.36 m
second link length	0.24 m
c.g. of base link from base motor axis	0.139 m
c.g. of 2nd link from 2nd motor axis	0.099 m
Coulomb friction of base axis	5.7 N·m
Coulomb friction of 2nd axis	0.9 N·m

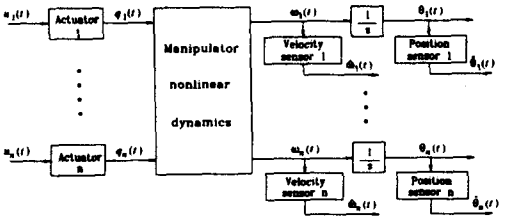

Fig. 1 Modelling structure of an n degree of freedom manipulator system

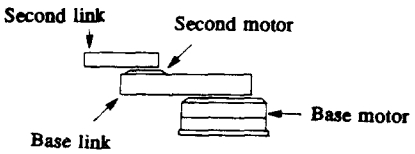

Fig.2 Schematic picture of the Berkeley/NSK mainpulator

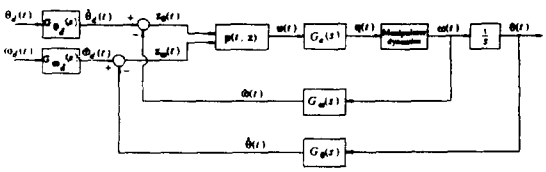

Fig. 3 Block diagram of the control system

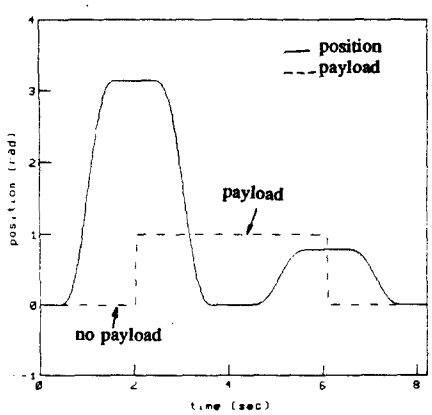

Fig. 4 Desired trajectory and payload changes simulating a pick-and-place task.

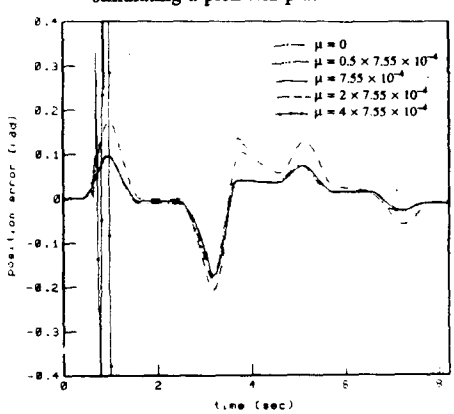

Fig. 5 Position tracking errors of the base axis when Q = diag(180,5,135,0.1), $\gamma_0 = 0.013$, $\gamma_1 = 1$, $\varepsilon = 80$ and $\rho = 100$; continuous time control; no payload

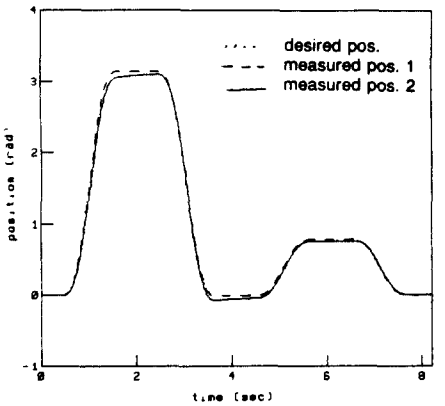

Fig. 6 Position trackings when Q = diag(16000,5,170,0.1), $\gamma_0 = 0.13$, $\gamma_1 = 5.8$, $\varepsilon = 40$ and $\rho = 50$; discretized control; no payload; computational delay; simulation

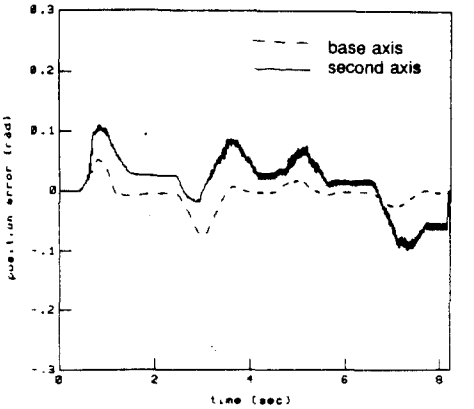

Fig. 9 Position tracking errors (desired pos.- measured pos.); discretized control; no payload; experiment

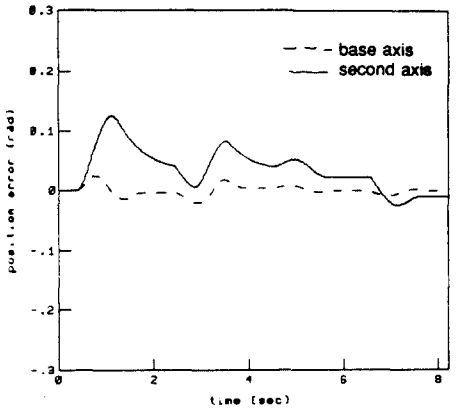

Fig. 7 Position tracking errors (desired pos.- measured pos.); discretized control; no payload; computational delay; simulation

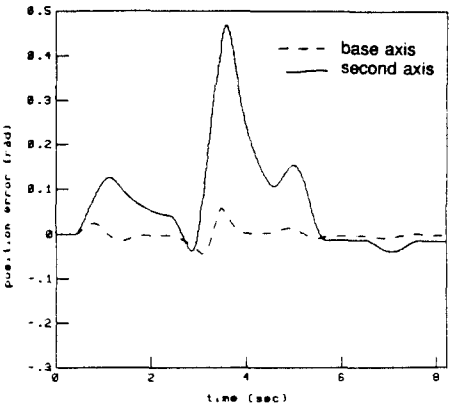

Fig. 10 Position tracking errors (desired pos.- measured pos.); discretized control; payload; computational delay; simulation

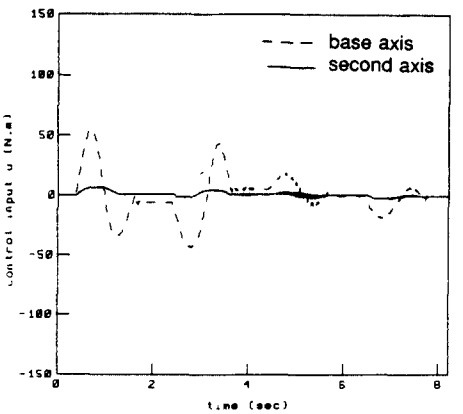

Fig. 8 Control inputs; discretized control; no payload; computational delay; simulation

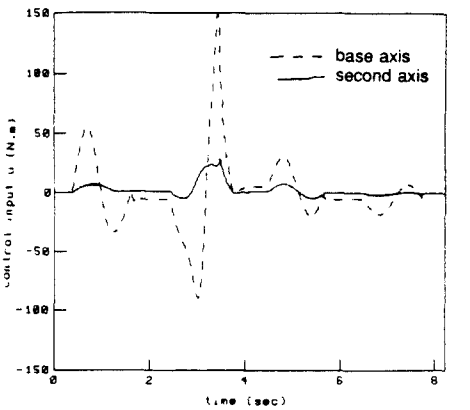

Fig. 11 Control inputs; discretized control; payload; computational delay; simulation